Quasi-hydrophilic black silicon photocathodes with inverted pyramid arrays for enhanced hydrogen generation

Shuai Zhao,[ab] Guodong Yuan,*[ab] Qi Wang,[ab] Wenqiang Liu,[ab] Ru Wang[c] and Shenghua Yang[c]

[a] *State Key Laboratory for Superlattices and Microstructures, Institute of Semiconductors, Chinese Academy of Sciences, Beijing 100083, China.*

[b] *Center of Materials Science and Optoelectronics Engineering, University of Chinese Academy of Sciences, Beijing 100049, China.*

[c] *School of Electronic Information Engineering, Hebei University of Technology, Tianjin 300130, China.*

*Author to whom correspondence should be addressed. Email: gdyuan@semi.ac.cn

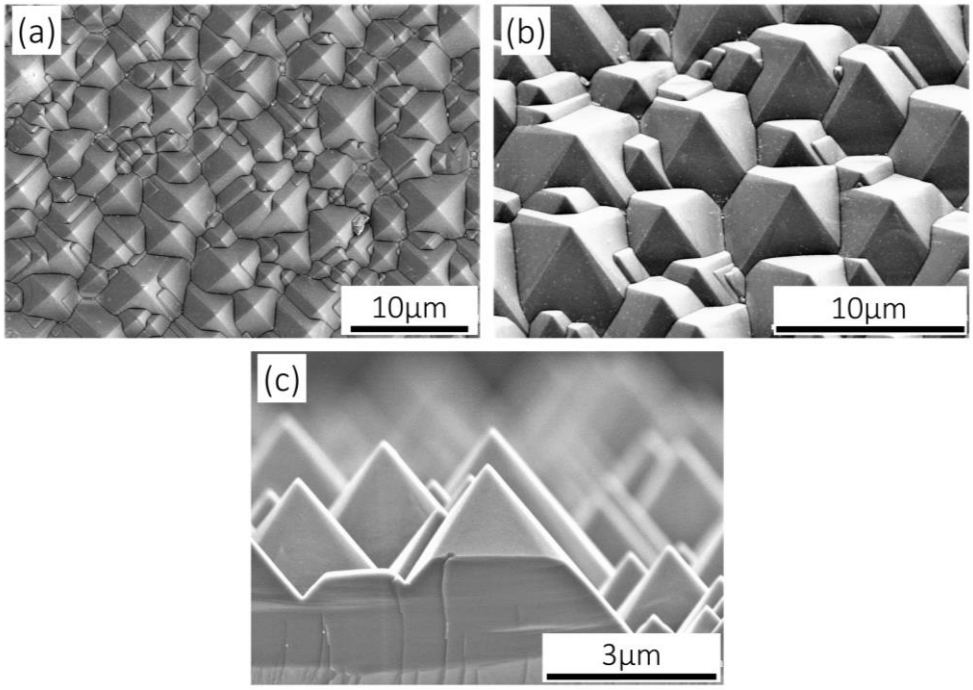

Fig. S1. Microscopy of SiUPs wafers. (a) Plan-view, (b) 25°-tilted plan-view, and (c) cross-sectional SEM images of SiUPs wafers.

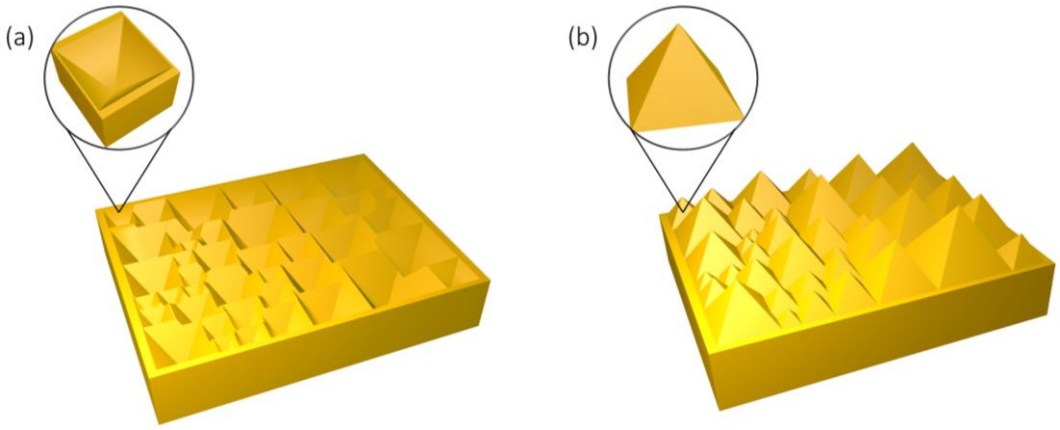

Fig. S2. Three-dimensional schematic illustrations for etched Si surfaces. (a) Sunk etching pits of SiIPs. (b) Projecting bulges of SiUPs.

Table S1. Effective minority carrier lifetimes (μs) for etched Si wafers.

	Average	Median	Std. Dev.	Min.	Max.
SiUPs	0.99	0.99	0.00	0.98	0.99
SiNWs	0.61	0.61	0.00	0.60	0.61
SiIPs	0.93	0.93	0.00	0.92	0.93

Experimental details for the effective minority carrier lifetime measurements:

Textured Si wafers were dipped into buffered oxide etch solutions for 2 h to remove etching-induced oxide layers and native oxide layers. Subsequently, these wafers were repeatedly rinsed with deionized water and then dried by nitrogen. All the wafers were put into the WT-2000 lifetime tester working at the μ-PCD (non-contact microwave photoconductance decay) mode thereafter. Measured effective minority carrier lifetimes (μs, one sun) are shown in Table S1.

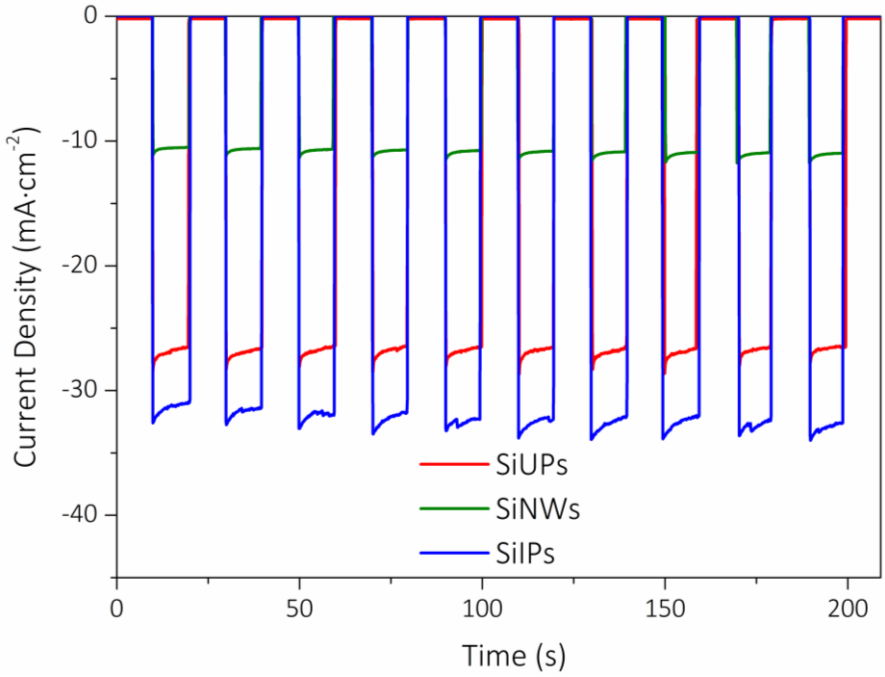

Fig. S3. J-t curves of textured p-Si photocathodes at -0.85 V *vs.* RHE under chopped one sun illumination.

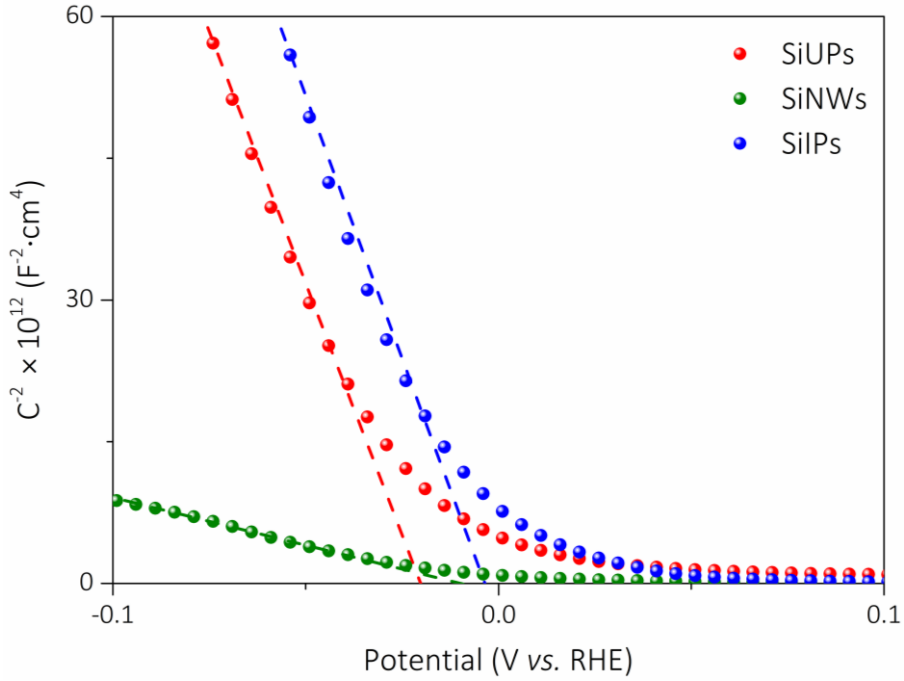

Fig. S4. MS plots obtained *via* impedance-potential experiments for textured p-Si photocathodes. Dash lines are the linear fitting results for corresponding measured data.

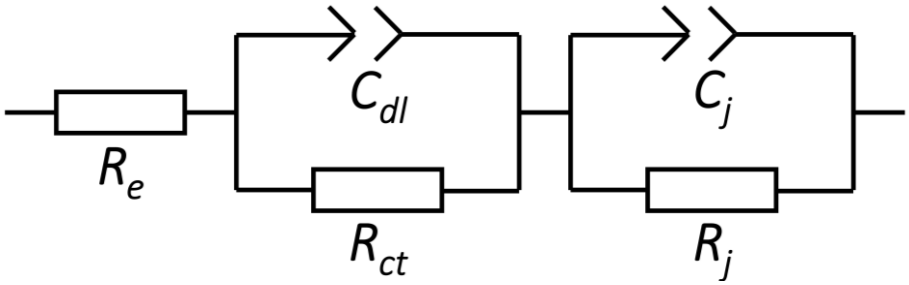

Fig. S5. A schematic diagram for the equivalent circuit model applied in EIS data fitting.

CoS_2 is an intrinsically metallic material without band gap, and thus we can assume that no depletion layers and corresponding micro-capacitive components exist at the CoS_2/electrolyte interfaces. Therefore, this equivalent circuit model was not only used to fit the EIS data for three patterned bare-Si photocathodes under a low or high reverse bias voltage (Fig. 3b and d), but for the SiIPs/CoS_2 ones (Fig. 7a). As for the SiIPs/CoS_2 cathodes, C_j and R_j, the "junction-related" components, respectively represent the equivalent capacitance and resistance of multiple parallel Si/electrolyte and Si/CoS_2 junctions.

Table S2. Fitting results of EIS data for textured Si photocathodes.

	R_e(Ω·cm^2)	C_{dl}(μF·cm^{-2})	R_{ct}(Ω·cm^2)	C_j(μF·cm^{-2})	R_j(Ω·cm^2)
SiUPs (-0.05 V)	21.94	14.4	344.6	24.45	10.93
SiNWs (-0.05 V)	35.05	71.74	735.4	80.02	4.313
SiIPs (-0.05V)	20.42	15.08	756.1	126.6	7.285
SiUPs (-0.65 V)	8.913	38.3	4.703	0.2615	9.526
SiNWs (-0.65 V)	11.89	13.98	9.159	16.45	6.694
SiIPs (-0.65V)	10.44	10.11	7.17	76.48	8.158

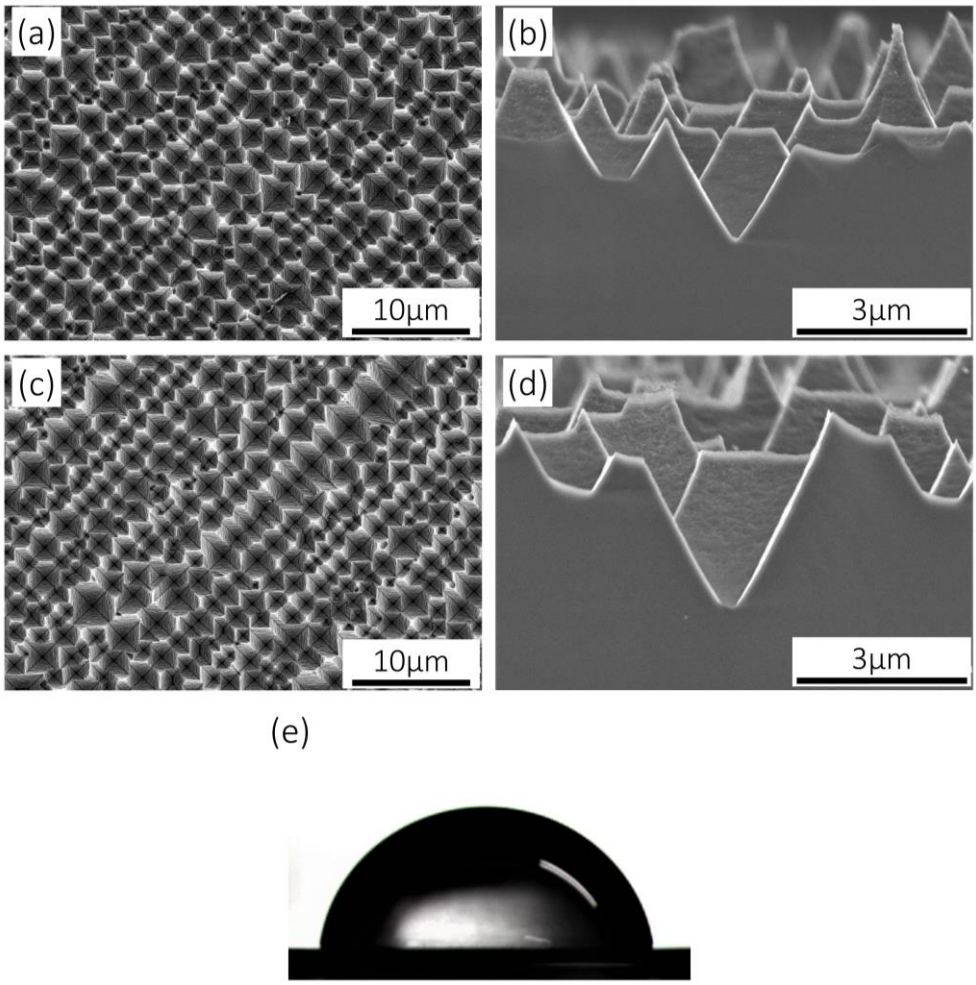

Fig. S6. Characterization for the stability of quasi-hydrophilic SiIPs photocathodes. (a,b) SEM images of as-synthesized SiIPs photocathodes. (c,d) SEM images and (e) water droplet contact shape of SiIPs photocathodes after an 8000 s-long bulk electrolysis at -0.5 V (*vs.* RHE) in aqueous H_2SO_4 solution (pH = 1) under one sun illumination.

There are no obvious morphological differences between the SiIPs cathodes before and after an 8000 s-long bulk electrolysis. After such HER measurements, the SiIPs cathode still possesses a water droplet contact angle of ~91° and remains quasi-hydrophilic.

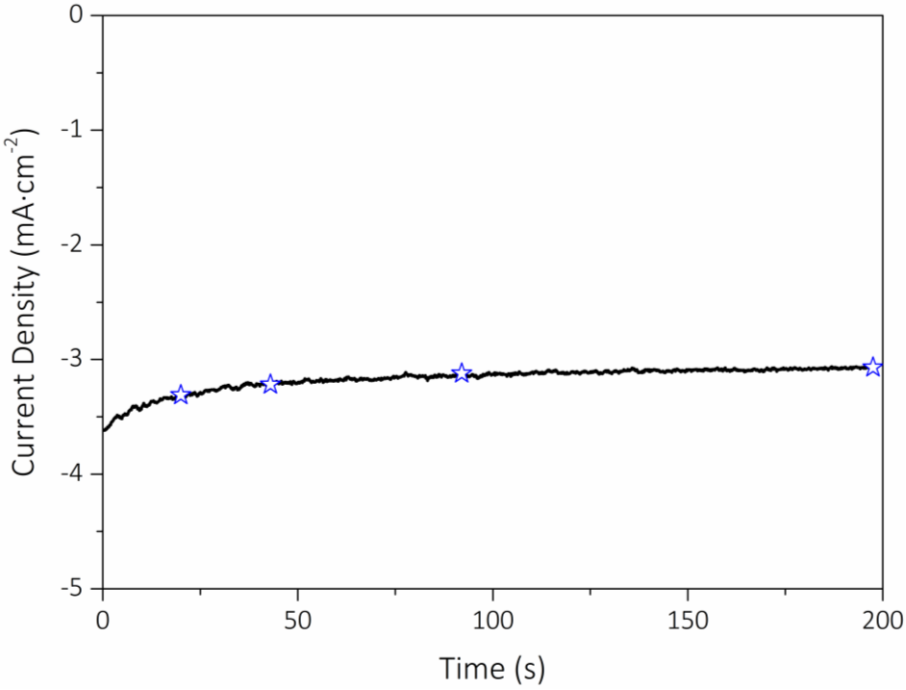

Fig. S7. A typical J-t curve during potentiostatic Co electrodepositions.

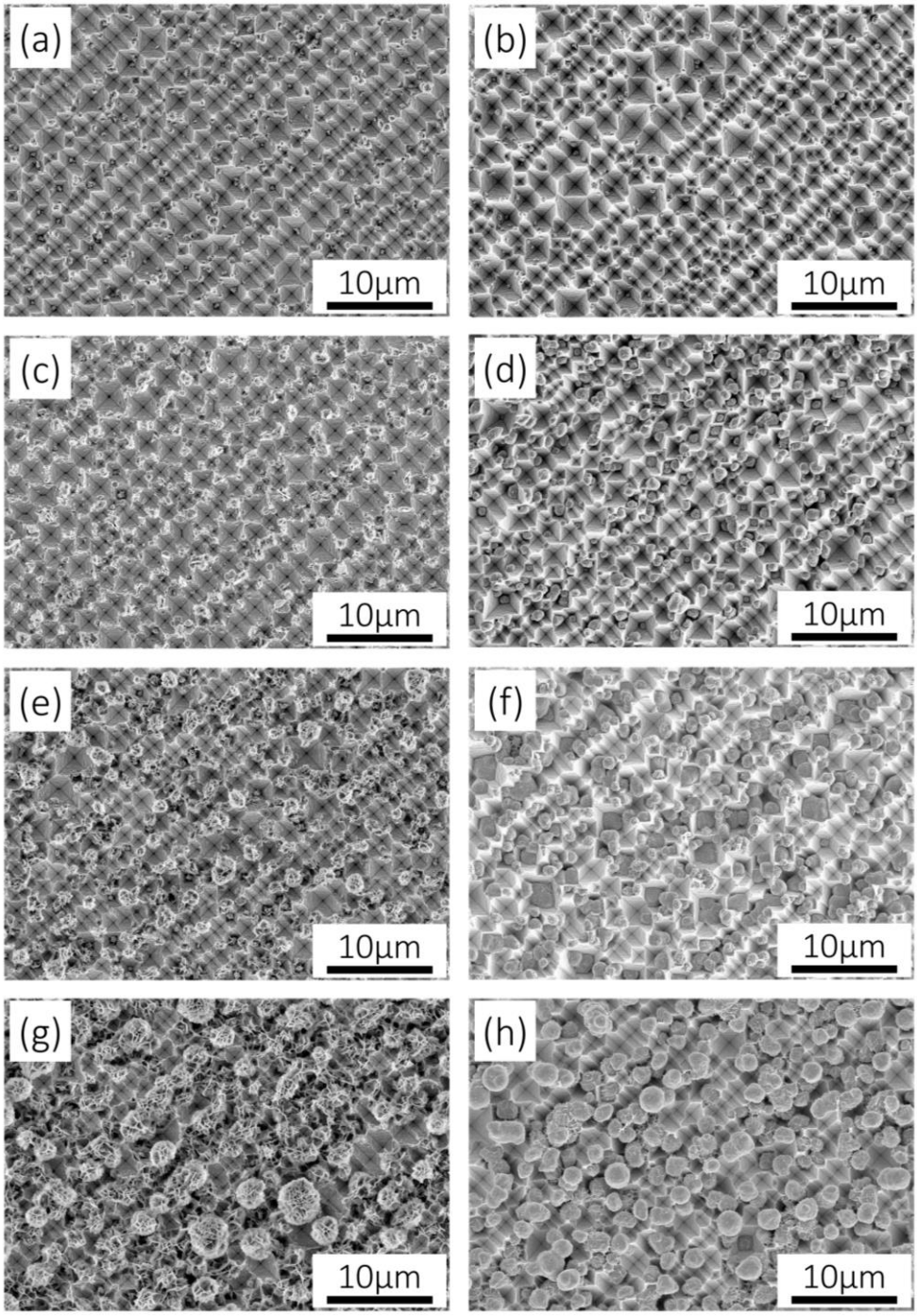

Fig. S8. Microscopy of as-prepared Co nanosheets/nanoflowers and CoS_2 nanocrystals on SiIPs wafers. (a,c,e,g) SEM images of Co-coated SiIPs wafers. The Co deposition charge densities are 50, 100, 200 and 400 $mC \cdot cm^{-2}$, respectively. (b,d,f,h) SEM images of SiIPs/CoS_2-50, 100, 200, 400 samples, respectively.

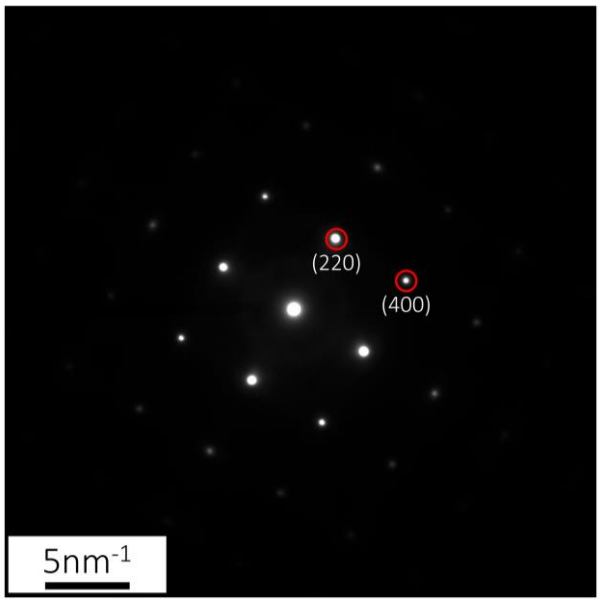

Fig. S9. Typical SAED patterns of etched SiIPs wafers.

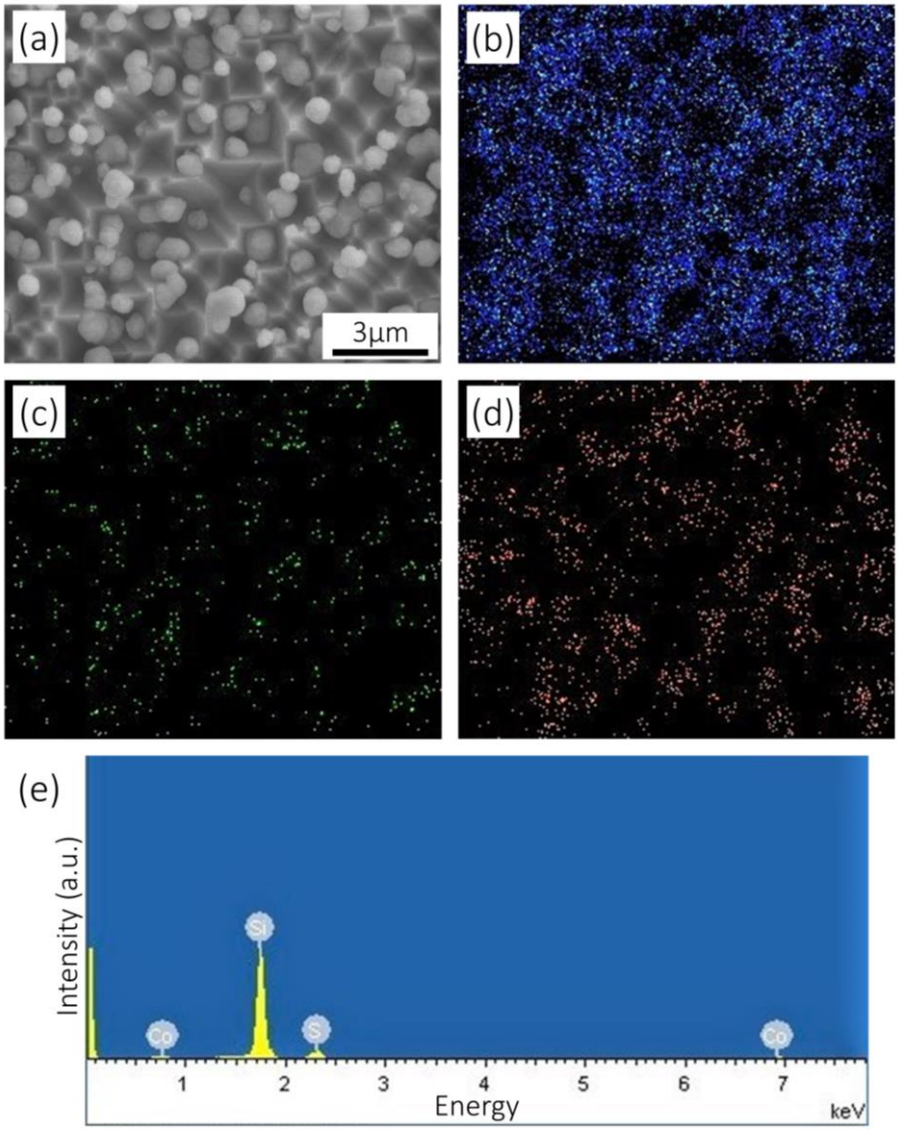

Fig. S10. EDX characterization of SiIPs/CoS_2 photocathodes. (a) A SEM image for the selected region, (b,c,d) EDX elemental mappings for Si, Co, S, respectively and (e) the EDX spectrum of the as-prepared SiIPs/CoS_2-200 photocathode.

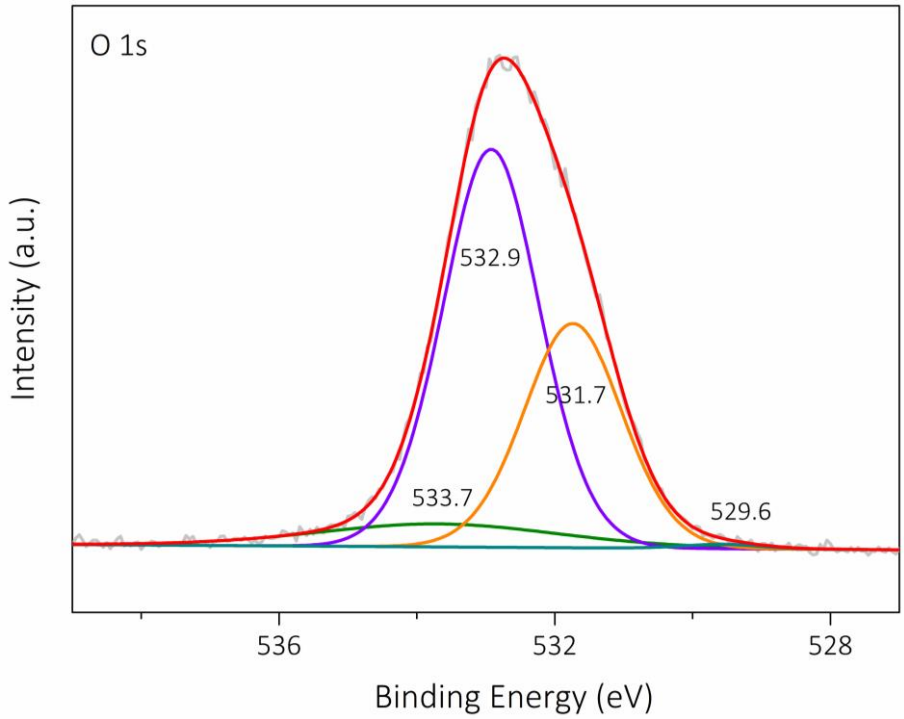

Fig. S11. XPS O *1s* spectrum of the SiIPs/CoS_2-200 photocathode.

In the XPS O *1s* spectrum, four deconvoluted peaks can be observed. The small peak centered at 529.6 eV indicates the presence of lattice oxygen (CoO_x), while two peaks at around 531.7 eV and 533.7 eV are derived from the terminal oxygen (hydroxyl) and absorbed water, respectively. Besides, the signature peak at 532.9 eV may be related to the native oxide layers of Si substrates.

Table S3. Fitting results of EIS data for Si/CoS_2 photocathodes.

	R_e(Ω·cm^2)	C_{dl}(μF·cm^{-2})	R_{ct}(Ω·cm^2)	C_j(μF·cm^{-2})	R_j(Ω·cm^2)
bare-SiIPs	20.42	15.08	756.1	126.6	7.285
SiIPs/CoS_2-50	25.61	14.9	453	1.875	4.065
SiIPs/CoS_2-100	20.49	14.07	294.4	4.851	4.315
SiIPs/CoS_2-200	13.03	9.852	169.4	6.829	3.23
SiIPs/CoS_2-400	14.95	13.46	110.3	9.971	2.719